

Ultrascaled Silicon Nanowires as Efficient Thermoelectric Materials

E. B. Ramayya and I. Knezevic

Electrical and Computer Engineering, University of Wisconsin, Madison, Wisconsin 53706

Email: ramayya@wisc.edu, knezevic@engr.wisc.edu

Abstract—The room-temperature thermoelectric figure of merit (ZT) of highly doped silicon nanowires (SiNWs) of square cross section was calculated by solving the electron and phonon Boltzmann transport equations with a proper account of the two dimensional confinement of both electrons and phonons. The ZT in SiNWs is almost two orders of magnitude larger than that of bulk silicon. The enhancement of ZT in SiNWs occurs primarily because of strong phonon-boundary scattering that degrades the lattice thermal conductivity by about two orders of magnitude from its value in bulk silicon. With decreasing wire cross section, the electrical conductivity (σ) and thermal conductivity (κ) decrease, whereas the Seebeck coefficient (S) increases. Therefore, the ZT variation with cross section is non-monotonic, with ZT maximal for a wire of cross section $4 \times 4 \text{ nm}^2$. Boundary roughness scattering indeed proves to have a significant effect on both electronic and thermal transport in SiNWs.

I. INTRODUCTION

Thermoelectric phenomena include conversion of electricity to heat and heat to electricity using solid state devices. A thermoelectric (TE) generator converts a temperature difference between two ends of a conductor into a bias voltage, whereas a TE refrigerator utilizes electrical current to create a temperature difference between two ends of a conductor (by pumping heat from cold end to hot end). Suitability of a material for thermoelectric applications at temperature T is judged from its figure of merit $ZT = S^2\sigma T/\kappa$, where S , σ , and κ are the Seebeck coefficient (thermopower), electrical conductivity, and thermal conductivity, respectively [1]. $S^2\sigma$ has to be as high as possible to ensure maximal conversion of electric power to heat and to minimize the Joule heating losses in the material, whereas thermal conductivity should be as small as possible to maintain the temperature gradient between the heat source and the heat sink (low κ will ensure that the heat is carried by the charge carriers from the source to the sink under the influence of the applied electric field rather than by the carriers diffusing in the opposite direction due to the presence of the thermal gradient). $ZT > 3.0$ (corresponds to about 20-30 % Carnot efficiency) is required to replace conventional chlorofluorocarbon (CFC) based coolers by TE coolers, but increasing ZT of bulk semiconductors beyond 1.0 has been a big challenge due to the interdependence of σ and S_e (the electronic contribution to the Seebeck coefficient). Unlike conventional refrigerators, which pollute the atmosphere because of CFC leaks, TE coolers are environmentally friendly. But TE devices are still not a commercially-viable alternative to conventional generators and coolers because of

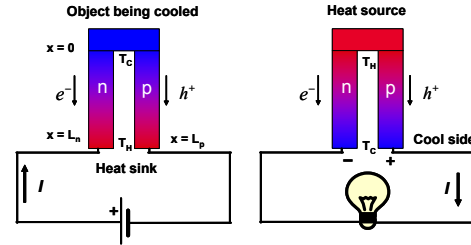


Fig. 1. Schematic of thermocouples used in thermoelectric (Peltier) coolers (left) and power generators (right). Thermoelectric devices are generally made of many thermocouples connected in parallel. The two legs of the couple are electrically in series but thermally in parallel.

their extremely low efficiency. At present, TE coolers are only used for niche applications (such as cooling laser diodes [2]) which require high reliability, small size, and light weight rather than high efficiency. In the future, TE generators could be used to tap the heat waste generated in automobiles to make automobiles more efficient, or power parts of integrated circuits [3].

In low-dimensional nanostructures, power factor S^2 can be enhanced by tuning the Fermi level to be near the bottom of a subband, where the density of states is high [4]. Recently, it was experimentally demonstrated [5], [6] that the ZT of Si nanowires at room temperature can reach values of up to 0.6, a tremendous increase over the bulk Si ZT value of 0.01. These results are exciting as they demonstrate that all-silicon on-chip cooling might be possible. However, the mechanism behind the increase in ZT is not clear: Boukai *et al.* [6] attribute this increase to the phonon-drag (S_{ph}) contribution to the thermopower, whereas Hochbaum *et al.* [5] attribute the increase in ZT to a decrease in the lattice thermal conductivity (κ_l) by two orders of magnitude as a result of phonon scattering from the boundary-roughness features and point defects.

The effect of increasing spatial confinement on the variation of κ_l in nanostructures has been extensively studied over the past few years [7]–[10], but a reliable estimate of ZT also requires a thorough understanding of the size effects on the electronic portions of thermal conductivity, as well as of S and σ . Recent studies of the electron mobility in SiNWs show a non-trivial variation of the electron relaxation with decreasing SiNW dimensions [11], [12]. As electron relaxation determines the variation of S , κ_e , and σ , calculation of these

parameters by solving the electron Boltzmann transport equation (BTE) becomes very important. Our previous study [12]–[14] has also shown that both the acoustic phonon-electron and the acoustic phonon-acoustic phonon scattering rates are enhanced in SiNWs due to the acoustic phonon confinement in them [15], [16].

In this study, we present a detailed simulation of electronic and thermal transport in ultrascaled, highly doped silicon nanowires, surrounded by native oxide. Electronic states are found from a self-consistent Poisson-Schrödinger solver within the effective mass framework [12], [13]. Confined acoustic phonon dispersions are calculated from the elastic continuum equation with the free-standing boundary conditions [16], appropriate for Si surrounded by SiO₂ (SiO₂ is acoustically softer than Si). The modified dispersion is used in the calculation of scattering of acoustic phonons with electrons and other acoustic phonons. Transport of charge and heat is described by solving the BTE for both electrons and acoustic phonons. Our study shows that the observed increase in ZT in SiNWs occurs primarily because of the extremely low lattice thermal conductivity in them ($\approx 1\text{-}2 \text{ W m}^{-1} \text{ K}^{-1}$, almost two orders of magnitude smaller than that in bulk Si) due to strong phonon-boundary scattering.

II. THERMOELECTRIC COEFFICIENTS

Thermoelectric coefficients S , σ , and κ , required to calculate the ZT in a material, can be derived from the electron and phonon BTEs [17]. Previous theoretical studies of ZT [4], [18] in wires assume extreme quantum limit and a constant relaxation time obtained from the bulk mobility to calculate the electronic coefficients such as S_e , κ_e , and σ . But as indicated in our previous work [12], [14], neither of these assumptions are valid for the wire cross sections considered in this study. κ_l is calculated either by solving the BTE for phonons [7]–[9], or using molecular dynamics simulations [10].

A. Electrical Conductivity

The SiNWs for thermoelectric applications are ungated and very highly doped to increase the electrical conductivity. In this study, the cross section of the SiNW is varied from $3 \times 3 \text{ nm}^2$ to $8 \times 8 \text{ nm}^2$ and the wire is surrounded on all sides by thermal oxide of thickness 1 nm. In obtaining the self-consistent wavefunctions and potential, the electric field and the wavefunctions are forced to zero at the air-SiO₂ interfaces. The silicon channel is assumed to be n-type doped to $1.6 \times 10^{19} \text{ cm}^{-3}$ with arsenic. Due to the high doping concentration, scattering from ionized impurities is expected to play a crucial role in determining the σ . So, apart from surface roughness scattering (SRS) and phonon scattering considered in our previous work [12], [13], [17], scattering due to impurities is also included in the calculation of σ . The derivation and the expressions used for the SRS and phonon scattering rates can be found in Ref. [12] and the expression for the electron-impurity scattering rate is derived in the Appendix.

Since the doping level is in the degenerate limit, the Pauli exclusion principle is included in the Monte Carlo simulation.

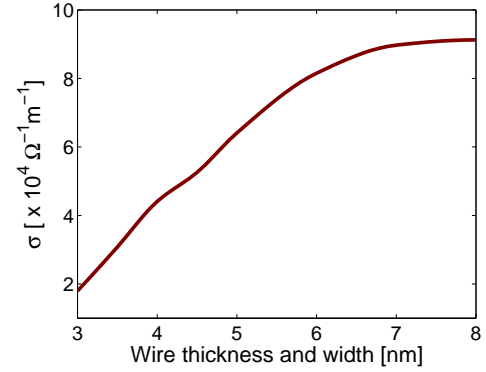


Fig. 2. Electrical conductivity in square SiNWs as a function of the wire cross section. The rapid drop in conductivity for wires of cross section below $5 \times 5 \text{ nm}^2$ occurs because of a significant increase in surface roughness scattering in ultra-small wires [19]. The doping density is $1.6 \times 10^{19} \text{ cm}^{-3}$.

It is incorporated by checking if the final state is empty or not before each scattering. The electron is allowed to undergo the scattering only if the final state is empty, if not, the scattering event is treated as a self-scattering [20]. Electrical conductivity in SiNWs decreases with the decrease in wire cross section (Fig.2). For relatively large wires, the impurity scattering and phonon scattering dominate the electrical transport, whereas for ultra-small wires the dominant contribution to the reduction in σ comes from the strong increase in the confinement-induced part of the surface roughness scattering [12].

B. Thermal Conductivity

Following the Klemens-Callaway method, the lattice thermal conductivity is calculated by solving the phonon BTE under the relaxation time approximation (RTA). κ_l for a SiNW with a square cross section is given by [21]

$$\kappa_l(T, a, \alpha) = \frac{k_B}{2\pi^2} \left(\frac{k_B T}{\hbar} \right)^3 \times \int_0^{\theta_D/T} \frac{x^4 e^x}{(e^x - 1)^2} \frac{\tau(x)}{\bar{v}(x)} \mathcal{L}[\gamma(x), \alpha] dx, \quad (1)$$

where $x = \hbar\omega/k_B T$, ω is the frequency of the phonon, θ_D is the Debye temperature, $\gamma(x) = a/\Lambda(x)$ is the ratio the NW side length a and the phonon mean free path $\Lambda(x) = \bar{v}(x)\tau(x)$, \bar{v} is the acoustic phonon group velocity averaged over all modes, $\tau(x)$ is the relaxation time of the acoustic phonon due to three-phonon Umklapp (τ_u), boundary scattering (τ_b), impurity scattering (τ_i), and electron scattering (τ_e), and \mathcal{L} defines the boundary scattering in NWs with square cross section. $0 \leq \alpha \leq 1$ is the fraction of specular reflection of phonons from the SiNW boundaries ($\alpha = 0$ indicates fully diffusive scattering). The expression for τ_u and τ_b were taken from Ref. [22] and τ_i and τ_e were taken from Ref. [23] and Ref. [15], respectively. For M acoustic phonon modes, the averaged group velocity is given by $\bar{v}(x) = 1/M \sum_n v_n(x)$.

κ_l variation with the wire cross section with fully diffusive boundary scattering is shown in the bottom panel of Fig. 3. κ_l decreases almost linearly with decreasing wire cross section

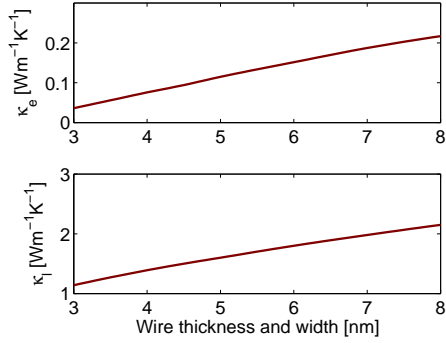


Fig. 3. Electrical (top) and phononic (bottom) components of thermal conductivity as a function of the SiNW cross section. As in bulk silicon, phonons dominate the lattice thermal conductivity. Thermal conductivity in SiNWs is almost two orders of magnitude smaller than that in bulk silicon because of strong phonon-boundary scattering.

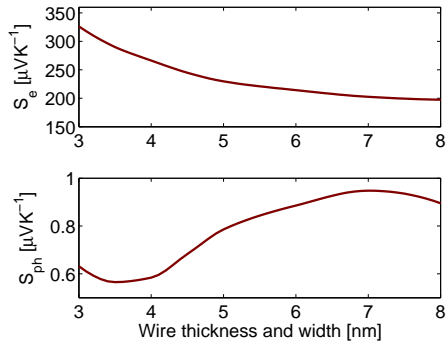


Fig. 4. Electronic (top) and phonon-drag (bottom) components of the Seebeck coefficient as a function of the SiNW cross section. The electronic component of the Seebeck coefficient is more than two orders of magnitude greater than the phonon-drag component.

due to a strong increase in both phonon-boundary and three-phonon scattering with decreasing wire cross section. The κ_l calculated in SiNWs shows a almost 70-fold decrease from its value in bulk silicon. But still it is almost two times larger than what has been observed experimentally. Better model needs to be developed to properly account for the large reduction in κ_l that was reported in Ref. [5], [6]. As in bulk semiconductors, the electronic portion of thermal conductivity is proportional to the electrical conductivity and therefore κ_e decreases with the decrease in the wire cross section (Fig. 3, top panel). κ_e has a negligible effect on the total thermal conductivity in SiNWs.

C. The Seebeck Coefficient

The phonon drag component of the Seebeck coefficient is due to the preferential scattering of phonons by electrons in the direction of current flow [24]. The phononic contribution to S is calculated from the fraction of the electron-acoustic phonon scattering rate to the total electron scattering rate (x), velocity of acoustic phonons (v_{ph}), relaxation time of acoustic phonons (τ_{ph}), and the mobility of electrons (μ). S_{ph} is given

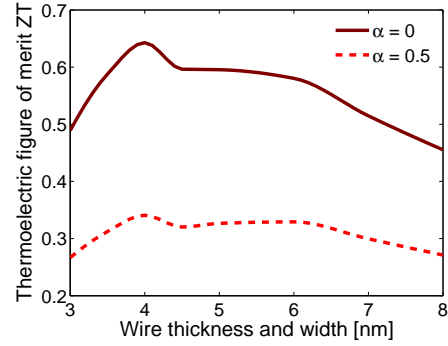


Fig. 5. ZT variation with the SiNW cross section. $\alpha = 0$ and $\alpha = 0.5$ correspond to 100 % and 50 % diffuse scattering of phonons at the boundaries. The ZT of rough SiNWs shows up to a 70-fold increase over the ZT of bulk silicon, and it drops rapidly for extremely small wire cross sections due to the strong reduction in electrical conductivity.

by

$$S_{ph} = \frac{xv_{ph}^2\tau_{ph}}{\mu T}. \quad (2)$$

v_{ph} is the average of $\bar{v}(\omega)$ over all ω , weighted by the Bose-Einstein phonon occupation number $N(\omega)$.

With decreasing wire cross section, x and τ_{ph} (see Eq. 2) decrease monotonically, because of the increase in the contribution of electron scattering from surface roughness, and the increase in phonon-phonon and phonon-boundary scattering, respectively. The interplay of these two variations with the mobility variation (proportional to σ) determines the S_{ph} variation shown in the bottom panel of Fig. 4.

The electronic component of the thermopower quantifies the electric field that opposes the diffusion of electrons from the hot side to the cold side. This electric field opposes the applied field in case of a TE cooler so it reduces the electrical conductivity, therefore S_e drops as σ increases (Fig. 4, top panel).

The thermoelectric figure of merit in SiNWs of cross sections $8 \times 8 \text{ nm}^2$ to $3 \times 3 \text{ nm}^2$ at room temperature is shown in Fig. 5. Except for extremely small wires, the ZT increases with decreasing wire cross section. Among the wires considered ZT reaches a maximum value of 0.65 for a wire of cross section $4 \times 4 \text{ nm}^2$. The ZT values obtained in this work are about six times larger than those in gated (nearly undoped) wires considered in our previous work [17].

III. CONCLUSION

An electrothermal simulator has been developed to solve the electron and phonon Boltzmann transport equations and is used to calculate the thermoelectric figure of merit in SiNWs. ZT in SiNWs is found to be 50-70 times higher than that in bulk silicon because of a drastic reduction in their thermal conductivity with increasing spatial confinement.

- As in bulk semiconductors, in SiNWs, the Seebeck coefficient is solely determined by the electrons and phonons dominate the thermal conduction.

- Both electrical and thermal conductivity decrease with decreasing wire cross section. Compared to the bulk value, the decrease in thermal conductivity is several times larger than the decrease in electrical conductivity.
- It becomes extremely important to account for the quasi-one-dimensional nature of both phonons and electrons to properly model ZT in SiNWs.

ACKNOWLEDGMENT

This work has been supported by the National Science Foundation through the UW MRSEC (DMR-0520527) and by AFOSR (FA9550-09-1-0230).

APPENDIX

Coulomb potential due to an ionized impurity of charge Ze , located at $\mathbf{R}(y_0, z_0)$ from the center of the wire cross section, felt by an electron at position $(\mathbf{r}(y, z), x)$ is given by

$$U(\mathbf{r}, x) = -\frac{Ze^2}{4\pi\epsilon_{si}\sqrt{(\mathbf{r}-\mathbf{R})^2+x^2}}e^{-\frac{\sqrt{(\mathbf{r}-\mathbf{R})^2+x^2}}{L_d}}, \quad (3)$$

where ϵ_{si} is the dielectric constant of silicon and $L_d = \sqrt{\frac{\epsilon_{si}k_B T}{e^2 N_a}}$ is the screening length for a doping density of N_a . The matrix element for the impurity-electron scattering can be written as

$$M_{nm}(\mathbf{k}_x, \mathbf{k}'_x) = -\frac{Ze^2}{4\pi\epsilon_{si}} \iint \psi_n(y, z) \times \left[\frac{1}{L_x} \int \frac{e^{i(k_x - k'_x)x} e^{-\frac{\sqrt{(\mathbf{r}-\mathbf{R})^2+x^2}}{L_d}}}{\sqrt{(\mathbf{r}-\mathbf{R})^2+x^2}} dx \right] \psi_m(y, z) dy dz. \quad (4)$$

Defining $q = |\mathbf{k}_x - \mathbf{k}'_x|$,

$$K_0(q, \mathbf{R}) = \int \frac{e^{iqx} e^{-\frac{\sqrt{(\mathbf{r}-\mathbf{R})^2+x^2}}{L_d}}}{\sqrt{(\mathbf{r}-\mathbf{R})^2+x^2}} dx, \quad (5)$$

$$I_{nm}(q, \mathbf{R}) = \iint \psi_n(y, z) K_0(q, \mathbf{R}) \psi_m(y, z) dy dz, \quad (6)$$

and \mathcal{E} and \mathcal{E}' as the initial and final energies of the scattered electron in the parabolic band approximation, the scattering rate from a single impurity using Fermi's Golden Rule is

$$\Gamma_{nm}^i(\mathbf{k}_x) = \frac{2\pi}{\hbar} \frac{Z^2 e^4}{16\pi^2 \epsilon_{si}^2 L_x^2} \sum_{k'_x} I_{nm}^2(q, \mathbf{R}) \delta(\mathcal{E} - \mathcal{E}'). \quad (7)$$

The total impurity-electron scattering rate due to an uniform doping density of N_a is obtained by integrating over the position \mathbf{R} of the dopants

$$\Gamma_{nm}^{imp}(\mathbf{k}_x) = \frac{Z^2 e^4}{16\pi^2 \hbar \epsilon_{si}^2 L_x} \int d\mathbf{R} N_a L_x \int dk'_x I_{nm}^2(q, \mathbf{R}) \delta(\mathcal{E} - \mathcal{E}') \quad (8)$$

Adding a nonparabolicity factor α and converting the dk'_x integration to $d\mathcal{E}'$ integration, the Eq. (8) becomes

$$\Gamma_{nm}^{imp}(\mathbf{k}_x) = \frac{Z^2 e^4 N_a \sqrt{m}}{16\sqrt{2}\pi^2 \hbar^2 \epsilon_{si}^2} \frac{(1 + 2\alpha\mathcal{E}_f)}{\sqrt{\mathcal{E}_f(1 + \alpha\mathcal{E}_f)}} \int d\mathbf{R} I_{nm}^2(q_x^\pm, \mathbf{R}). \quad (9)$$

where \mathcal{E}_f is the final kinetic energy defined in Ref. [12] and $q_x^\pm = k_x \pm k'_x$ is the difference between the initial and final electron wavevectors as defined in the SRS derivation.

REFERENCES

- [1] E. Altenkirch, *Physikalische Zeitschrift*, vol. 12, p. 920, 1911.
- [2] M. Labudovic and J. Li, "Modeling of TE cooling of pump lasers," *IEEE Trans. Compon. Packag. Tech.*, vol. 27, p. 724, 2004.
- [3] H. J. Goldsmid, *Thermoelectric Refrigeration*. Plenum, New York, 1964.
- [4] L. D. Hicks and M. Dresselhaus, "Thermoelectric figure of merit of a one-dimensional conductor," *Phys. Rev. B*, vol. 47, p. 16631, 1993.
- [5] A. I. Hochbaum, R. Chen, R. Delgado, W. Liang, E. Garnett, M. Najarian, A. Majumdar, and P. Yang, "Enhanced thermoelectric performance of rough silicon nanowires," *Nature*, vol. 451, p. 163, 2008.
- [6] A. I. Boukai, Y. Bunimovich, J. Tahir-Kheli, J. Yu, W. A. G. III, and J. R. Heath, "Silicon nanowires as efficient thermoelectric materials," *Nature*, vol. 451, p. 168, 2008.
- [7] A. Khitun, A. Balandin, and K. L. Wang, "Modification of the lattice thermal conductivity in silicon quantum wires due to spatial confinement of acoustic phonons," *Superlattices and Microstructures*, vol. 26, no. 3, p. 181, 1999.
- [8] N. Mingo, L. Yang, D. Li, and A. Majumdar, "Predicting the thermal conductivity of Si and Ge nanowires," *Nano. Lett.*, vol. 3, pp. 1713–1716, 2003.
- [9] D. Lacroix, K. Joulain, D. Terris, and D. Lemonnier, "Monte Carlo simulation of phonon confinement in silicon nanostructures: Application to the determination of the thermal conductivity of silicon nanowires," *Appl. Phys. Lett.*, vol. 89, no. 10, p. 103104, 2006.
- [10] I. Ponomareva, D. Srivastava, and M. Menon, "Thermal conductivity in thin silicon nanowires: Phonon confinement effect," *Nano Lett.*, vol. 7, no. 5, p. 1155, 2007.
- [11] S. Jin, M. V. Fischetti, and T. Tang, "Modeling of electron mobility in gated silicon nanowires at room temperature: Surface roughness scattering, dielectric screening, and band nonparabolicity," *J. Appl. Phys.*, vol. 102, no. 8, p. 083715, 2007.
- [12] E. B. Ramayya, D. Vasileska, S. M. Goodnick, and I. Knezevic, "Electron transport in silicon nanowires: the role of acoustic phonon confinement and surface roughness scattering," *J. Appl. Phys.*, vol. 104, no. 6, p. 1, 2008.
- [13] —, "Electron mobility in silicon nanowires," *IEEE Trans. Nanotechnol.*, vol. 6, no. 1, p. 113, 2007.
- [14] —, "Cross-sectional dependence of electron mobility and lattice thermal conductivity in silicon nanowires," *J. Comput. Electron.*, vol. 7, p. 319, 2008.
- [15] J. Zou and A. Balandin, "Phonon heat conduction in a semiconductor nanowire," *J. Appl. Phys.*, vol. 89, no. 5, p. 2932, 2001.
- [16] N. Nishiguchi, Y. Ando, and M. N. Wybourne, "Acoustic phonon modes of rectangular quantum wires," *J. Phys.: Condens. Matter*, vol. 9, p. 5751, 1997.
- [17] E. B. Ramayya, D. Vasileska, S. M. Goodnick, and I. Knezevic, "Thermoelectric properties of silicon nanowires," *Proceedings of the 8th International Conference on Nanotechnology*, p. 339, 2008.
- [18] A. W. T. M. Vo, V. Lordi, and G. Galli, "Atomistic design of thermoelectric properties of silicon nanowires," *Nano Lett.*, vol. 8, no. 4, p. 1111, 2008.
- [19] E. B. Ramayya and I. Knezevic, *in preparation*, 2009.
- [20] P. Lugli and D. Ferry, "Degeneracy in the ensemble Monte Carlo method for high-field transport in semiconductors," *IEEE Trans. Electron Devices*, vol. ED-32, no. 11, p. 2431, 1985.
- [21] X. Lü and J. Chu, "Lattice thermal conductivity in a silicon nanowire with square cross section," *J. Appl. Phys.*, vol. 100, no. 1, p. 014305, 2006.
- [22] X. Lü, J. H. Chu, and W. Z. Shen, "Modification of the lattice thermal conductivity in semiconductor rectangular nanowires," *J. Appl. Phys.*, vol. 93, no. 2, p. 1219, 2003.
- [23] M. Asheghi, K. Kurabayashi, R. Kasnavi, and K. Goodson, "Thermal conduction in doped single-crystal silicon films," *J. Appl. Phys.*, vol. 91, p. 5079, 2002.
- [24] G. Nolas, J. Sharp, and J. Goldsmid, *Thermoelectrics: Basic Principles and New Materials Developments*. Springer, New York, 2001.